

# Variability of Ocean Features and their Impact on Cyclogenesis over Arabian Sea During Post Monsoon Season

suchandra Aich Bhowmick (✉ [suchandra81@yahoo.com](mailto:suchandra81@yahoo.com))

Space Applications Centre <https://orcid.org/0000-0002-7466-1982>

Anup Mandal

Indian Space Research Organization

---

## Research Article

**Keywords:** Arabian Sea, North Indian Ocean, South West Indian Ocean, sea surface carbon over AS

**Posted Date:** June 23rd, 2021

**DOI:** <https://doi.org/10.21203/rs.3.rs-610731/v1>

**License:**   This work is licensed under a Creative Commons Attribution 4.0 International License.

[Read Full License](#)

---

# Variability of ocean features and their impact on cyclogenesis over Arabian Sea during post monsoon season

Suchandra A. Bhowmick<sup>@</sup> and Anup Kumar Mandal  
Oceanic Sciences Division, Atmospheric and Oceanic Sciences Group,  
Space Applications Centre, ISRO  
Ahmedabad 380015, India

Arabian Sea (AS), the western sector of North Indian Ocean (NIO) produce smaller number of tropical cyclones as compared to Bay of Bengal. Though limited in numbers, the cyclones over Arabian sea are catastrophic by character. This make west coast of Indian subcontinent vulnerable to these hazards. The post-monsoon cyclogenesis over this region is known to be modulated by both monsoon rainfall and the El-Niño accompanied with positive Indian Ocean Dipole events. No single phenomena, however, can fully explain the variability observed in AS region.

In this study, it is observed that apart from several known atmospheric forcings, inter-annual variability of ocean heat content (OHC) influence the post-monsoon AS cyclogenesis. The OHC of this region is partially modulated by the changes in salinity. Heat exchanges between the South West Indian Ocean (SWIO) and AS also modulates the OHC over AS. This remote influence is facilitated largely by the variability in the equatorial currents. Further it is seen that the recent trend of increased OHC post-2011 matches with the enhanced sea surface carbon over AS.

## 1. Introduction:

Arabian Sea (AS) which represents the western part of North Indian ocean (NIO), is relatively calm in terms of convective activities as compared to the eastern sector i.e. Bay of Bengal (BoB). Climatologically, more cyclones form in BoB as compared to inert AS (Sahoo and Bhaskaran 2016). This in-equal cyclogenesis is primarily because the ocean/atmospheric dynamics over these regions are entirely different. It is well known that atmosphere plays a critical role in cyclogenesis. Several studies like Ali et al 2013 and 2007, Shay et al 2000, Goni et al. 2003 etc also highlighted important role of ocean in modulation of cyclone track and intensity. In this paper emphasis is only on the ocean forcing for cyclogenesis over AS. The distribution asymmetry of cyclones between AS and BOB has been vividly discussed in Sattar and Cheung, 2019. An active convective season in AS is often associated with a less active convective season over BoB. This phenomenon is more pronounced in post monsoon months of October-December (Evan and Camargo, 2011; Sattar and Cheung, 2019). From ocean preview, BOB and AS are very different. Over BoB, active river discharge makes upper layer of the ocean fresh. This make the ocean stratified with shallow mixed layer depth (MLD). A stratified ocean retain heat in upper layers (Akhil et al 2014) making BoB a hotspot for cyclone formation.

---

Suchandra Aich Bhowmick

[suchandra81@yahoo.com](mailto:suchandra81@yahoo.com)

Oceanic Sciences Division, Atmospheric and Oceanic Sciences Group,  
Space Applications Centre, ISRO  
Ahmedabad 380015,India

46 AS, on the other hand have much less river discharge unlike BoB, making it more saline region  
47 that normally produce less number of cyclones. AS is known to be comparatively more active  
48 for cyclogenesis during the El-Niño years accompanied with positive phase of Indian Ocean  
49 Dipole (IOD) as compared to a simple El-Niño Years (Sumesh and Ramesh Kumar 2013). The  
50 seasonal distribution of the tropical cyclones over the Arabian Sea is bimodal. Cyclone  
51 formation peaks during pre-monsoon phase of May-June and during post-monsoon phase of  
52 October-December. During both these phases the cyclones causes the storm surges  
53 accompanied with large amplitude wind waves and tides. On an average 1-2 cyclones form  
54 over AS, most are intense enough to cause an impactful landfall. These makes AS cyclones  
55 hazardous for the west coast of India. (Murthy and Sabh 1984). In an interesting study Evan  
56 and Camargo (2011) showed that cyclones of May and June over AS are associated with early  
57 and late monsoon onset, respectively. The cyclones in November are associated with high sea  
58 level pressure over BoB. Thus, an active cyclonic season in AS implies non-occurrence in BoB.  
59 Off late in the post monsoon months, AS has shown a significant rise in the cyclonic activities.  
60 The persistence of AS cyclones from 2011 onwards makes the perception about its innerness  
61 quite precarious. Increasing cyclonic activity over AS was also linked to global warming by  
62 Prassana kumar et al 2009 and Murakami et al 2017. Albeit there are studies conducted on AS  
63 cyclone climatology and inter annual changes in environmental factors modulating  
64 cyclogenesis, yet studies discussing the inter-annual variability of physical and chemical  
65 properties of underlying oceans that may be important for changing behaviour of the AS is rare.

66 In this study, we observe the inter-annual changes of the Ocean Heat Content (OHC) are  
67 significantly correlated with variability of cyclogenesis over AS during the post monsoon  
68 month of Oct-Dec of 1979-2017. The study aims at better understanding of the ocean processes  
69 that could possibly contribute towards the variability of OHC in this region. OHC variability  
70 over AS is found to be influenced by the local changes in physical and chemical properties of  
71 ocean. One important local property is variability in freshening which is found to modulates  
72 OHC by regulating heating of the upper ocean. The phase of increased OHC over AS  
73 interesting matchup with higher partial pressure of sea surface carbon over Arabian sea. Heat  
74 exchange between the South Western Indian Ocean (SWIO) and AS is also an important aspect  
75 that influence OHC.

## 76 2. Data and Methods

77 We explore best track data from 1979-2019 available from U.S. Navy's Joint Typhoon  
78 Warning Centre (JTWC) to look into long term record of cyclones over AS. The mean  
79 precipitation over AS and adjoining SWIO was analysed to observe its dependence on ENSO  
80 events. This is done using Climate Prediction Centre (CPC) Merged Analysis of Precipitation  
81 (CMAP) data. Ocean salinity and temperature fields are taken from Ocean Re-Analysis  
82 (ORAS4) data provided by European Centre for Medium Range Weather Forecast (ECMWF).  
83 Using ORAS4, ocean heat content and its freshening is studied. Prior to its use, ORAS4 data  
84 is validated using temperature/salinity profiles from in-situ ARGOs. Observation based gridded  
85 monthly SPCO2 is used to analyse ocean carbon content and its correlation with SST. SST data used  
86 here is collected from ECMWF Reanalysis (ERA) interim datasets. A brief description of the data  
87 and methodology is provided below.

88 According to JTWC, over AS, total 88 cyclones formed during January-December of 1979-  
89 2019. Out of these, 27 were pre-monsoon (Apr-Jun) cyclones and 53 during post-monsoon  
90 (Oct-Dec). Our study strictly restricts to post monsoon phase. Best-track information of JTWC  
91 provide date/time of genesis and maximum sustained wind speed with locations. Cyclones vary

92 in terms of occurrence, intensity and duration. For determining inter-annual variability of  
 93 cyclone-intensity, one must consider all of these simultaneously. A decent way to do this is  
 94 computing accumulated cyclonic energy (ACE) for each cyclone of a year and then adding  
 95 them up. Mathematically ACE is represented in equation-1 below as:

$$\text{ACE} = 10^{-4} \sum V_{\max}^2 \quad (1)$$

96

98

99 The maximum wind speed ( $V_{\max}$ ) is considered till landfall. Some cyclones formed in BoB,  
 100 and after landfall crossed southern coast of India and came to AS. We have considered only  
 101 those data points which are in the AS (50°E-75°E,0°N-25°N). The ACE hence calculated is  
 102 used to study the inter-annual variability of cyclonic activity over AS. The years are categorized  
 103 as El-Niño, La-Niña or normal years based on the Oceanic Niño Index (ONI) defined by  
 104 NOAA. The ONI is used for detecting El Niño (warm) and La Niña (cool) events in the tropical  
 105 Pacific. It is the running 3-month mean SST anomaly for the Niño 3.4 region (i.e., 5°N–5°S,  
 106 120°–170°W). Events are defined as 5 consecutive overlapping 3-month periods at or above  
 107 the +0.5° anomaly for warm (El Niño) events and at or below the –0.5° anomaly for cold (La  
 108 Niña) events. (<http://ggweather.com/enso/oni.htm>). Further the classification of years on basis  
 109 of positive/negative Indian Ocean Dipole (IOD) events is taken bureau of meteorology  
 110 (bom.gov.au). Table -1a and b shows this year wise categorization. Rainfall over AS and  
 111 adjoining SWIO is modulated by these ENSO events. Inter-annual variability of rainfall over  
 112 this region corresponding to the El-Niño/La-Niña and phases of IOD is studied using the  
 113 CMAP data. CMAP data sets are monthly, global gridded precipitation at spatial resolution of  
 114 2.5°X2.5°. It contains gauge data along with five type of satellite based precipitation estimates  
 115 from Global Precipitation Index (GPI), OLR Precipitation Index (OPI), Special Sensor  
 116 Microwave/Imager (SSM/I) in scattering and emission mode and Microwave Sounding Unit  
 117 (MSU).

118  
 119 ORAS4 from ECMWF is valuable resource for climate variability studies available at 0.5°  
 120 spatial resolution from 1958-2017. It is based on a data-assimilative numerical ocean model  
 121 called Nucleus for European Modelling of the Ocean (NEMO). 3D-Variational data  
 122 assimilation technique ([Balmaseda et al. 2013](#)) is used for assimilation of altimeter data in this  
 123 model. Though, the data is temporally extensive yet the first two decades of the data has to be  
 124 used with caution. This is because of large uncertainties in absence of proper altimeter data. In  
 125 this study the surface/subsurface temperature, salinity and current information from this  
 126 reanalysis is extensively used in this study for the period of 1979-2017. ORAS4 has known  
 127 limitation of underestimating the Atlantic meridional circulation and having large errors in  
 128 surface salinity. Therefore, this data has been validated using the Argo profiles prior to its use.  
 129 ORAS4 temperature profiles has been used to compute the ocean heat content over the SWIO  
 130 and AS which is mathematically given as:

$$\text{Heat Content} = \int_0^D \rho C_p T dz$$

131  
 132 Here  $\rho$  is the density. Usually the density is salinity dependent, however for simplicity in  
 133 calculation this is taken constant over AS.  $C_p$  is the specific heat at a constant pressure and  $T$   
 134 is the temperature of  $dz$  is infinitesimal depth of water. The calculation is limited between the  
 135 surface to a depth  $D$ . One may consider  $D=2000\text{m}$  or even more. However, [Häkkinen et al.  
 136 2016](#) shows heat content up to 2000 m produces similar trend as that up to 700 m except for  
 137 higher amplitudes. Thus, in this case  $D$  is taken as 700m. Further to analyse the heat exchanges  
 138 between AS and SWIO, the meridional transport has been calculated using the ORAS4 data.  
 139 Here

140

$$\text{Meridional Transport} = \rho C_p \iint_0^{700} v T dx dz$$

141 where dx and dy represents the small interval of longitude and latitude respectively.

142 The observation based global monthly gridded sea surface partial carbon die oxide is available  
143 from Max Plank Institute from 1982-2019. The reanalysis is based on an artificial neural  
144 network and is available at 1X1° spatial resolution (Landschützer et al 2017). To understand  
145 the way carbon, influence the ocean heat, its correlation with SST is explored. The 6-hourly  
146 data of SST from ECMWF Reanalysis i.e. ERA Interim has been utilized. The data is available  
147 in real time mode. The duration of the data is 1979 onwards. The data assimilation system used  
148 to produce ERA interim datasets is based on 2006 release of IFS (cy31r2) with a 4D vibrational  
149 data assimilation scheme. The data is of high quality and extremely useful multivariate climate  
150 data set (Dee, 2011).

151

### 152 3. Validation of ORAS4

153 Since we have utilized ORAS4 temperature and salinity extensively for this study, a gross  
154 validation was carried out using in-situ measurements ARGO. Argo profile (ID-2901337)  
155 provided by Indian National Centre for Ocean Information Services (INCOIS) is used for the  
156 comparison of temperature and salinity profile for the year 2012. Choice of this validation year  
157 is not arbitrary. In this year the Argo data discontinuity was minimum. Argo observations,  
158 located within 0.5°x0.5° grid were taken into account to compute the average observed monthly  
159 temperature. The average of four data points from ORAS4 within 0.5°x0.5° grid were  
160 computed to obtain average ORAS4 temperature and then these were inter-compared. The  
161 Argo observations were also linearly interpolated till 700m depth along the Z-axis at same  
162 vertical grid points as in ORAS4 data. The observed monthly mean was computed by taking  
163 the time average of Argo data for a particular month. The position of the Argo was also  
164 computed by taking the average of Longitudes/Latitudes over a given month. The variation in  
165 position of Argo while it is moving in vertical direction for a time-step has not been considered,  
166 which may be possible source of error in observed temperature fields.

167

168 The comparison of ORAS4 and Argo temperature for different months in year 2012 is shown  
169 in Figure 1. Clearly the temperature of Argo and ORAS4 agree with one another. Up to 700m  
170 we find good match between the duos. The RMSE of month of August is maximum out of all  
171 months i.e. 0.73, however the correlation coefficient exceeds 99% for all months. When it  
172 comes to salinity (Figure 2), up to 200m the ORAS4 matches well with Argo. However, after  
173 200 m the salinity biases increases for AS. The surface salinity has a small bias for months of  
174 April, May and August; however, ORA is able to capture the largescale variability of the  
175 salinity over time. Therefore, while analysing the inter-annual variability of the salinity data  
176 from ORAs4, in this study we restrict ourselves to a depth between surface to 100m.

177

178

### 179 4. Results and Discussions

180 Long term post-monsoon precipitation over AS and adjoining areas like SWIO shows limited  
181 rainfall over Arabian Sea (AS) as compared to SWIO. CMAP monthly precipitation rate over  
182 the western part of Indian Ocean is shown in Figure 3. It clearly indicates that monthly averaged  
183 precipitation between 50°-70°E for October-December is high in SWIO. But towards AS, the  
184 precipitation decreases. Though limited in terms of occurrence, over AS these precipitation  
185 event has a strong inter-annual variability. Over SWIO the inter-annual variation of post  
186 monsoon rainfall rate between October to December and total 3 monthly precipitation rate has  
187 been shown in Figure 4. The years are classified into normal/El-Niño/La-Niña years

188 represented by black, red and green respectively. The combination of dash and dash-dots shows  
189 associated positive and negative phases of IOD. Very clearly, the precipitation is largely  
190 influenced by these air sea interaction processes. The years of El-Niño with a positive IOD has  
191 high precipitation over SWIO.

192 When we consider cyclonic events over neighbouring AS which contributes towards the mean  
193 precipitation of this region, such clear-cut conclusion cannot be drawn. AS has strong inter-  
194 annual variability in ACE as shown in [Figure 5](#). In this figure time series of ACE from 1979-  
195 2019 (41 years) has been shown. The years are further categorized into normal/El-Niño/La-  
196 Nina years with dash and dash-dots representing associated positive and negative phases of  
197 IOD. It is noteworthy to see that the variation in ACE is modulated with occurrences of El-  
198 Niño/La-Niña and positive and negative phases of IOD. Particularly El-Niño or a positive IOD  
199 or both together enhances the ACE to a great extent. The cyclonic activities over AS shows  
200 kind of persistence between 1992-1998 and 2003-2004. Of late however cyclonic activities  
201 over AS has gradually increased and it is more pronounced after 2011. Thus, it is evident that  
202 no single event can explain cyclogenesis over AS to the fullest. In this regard, ocean as a  
203 system is very less discussed. We thus systematically analyse, first the local ocean conditions  
204 over AS and then the conditions that persists in SWIO and equatorial Indian Ocean that can be  
205 remotely influence the AS cyclones.

206 In order to investigate the local ocean conditions, we analyse Ocean Heat Content (OHC) over  
207 the AS computed using Equation 2. The ORAs4 data is utilized for this purpose. The [Figure 6a](#)  
208 shows the OHC over AS from 1979-2017. The [Figure 6a indicates](#) increase in OHC of AS post  
209 2011. [The figure 6b shows the correlation coefficient between the OHC and ACE over AS.](#)  
210 [The correlation here is generated using a moving window of five consecutive years or a pentad.](#)  
211 [Clearly the correlation took over in the pentad from 2007-2011 and there on it increases](#)  
212 [monolithically. Thus OHC is undoubtedly the ocean parameter which plays key role in cyclone](#)  
213 [energies.](#)

214 It is well known that OHC is often modulated by freshening of the ocean. The fresh stratified  
215 layer with lower salinity, traps enormous heat in the upper layer of the ocean increasing the  
216 OHC. This process of stratified ocean trapping heat is much discussed for BOB. Thus,  
217 corresponding variability in salinity is analysed for AS too and is shown in the [Figure 7](#). Some  
218 of the quick look examples of such salinity modulated OHC are 1982, 1994, 1997 and 2015.  
219 In all these years salinity was less implying fresh upper layer of the ocean that can trap heat.  
220 This freshening could be a probable impact of good monsoon rainfall.

221 To a contrary, few noteworthy years of exceptions are also there. In these years freshening  
222 theory does not uphold. In 2004 salinity was comparable to 2015 but post –monsoon heat  
223 content was much less. In 2011, 2014, 2017 heat content was high enough, but salinity was  
224 also high. These exceptions are a clear-cut indication of an alternate forcing. To stepwise  
225 analyse these alternatives, we firstly considered the inter-annual variability of ocean surface  
226 carbon die oxide (CO<sub>2</sub>). [Figure -8](#) shows time series of anomaly of partial pressure of CO<sub>2</sub> at  
227 ocean surface. We can clearly infer from figure -8 that the partial pressure of the carbon has  
228 monotonically increased after 2011 with high positive anomaly. 2003 and 2004 also shows  
229 higher pCO<sub>2</sub> over AS. However, if these two are connected events or not is a matter of detailed  
230 study. To investigate this aspect, we analyse the SST from ERA interim data set and find the  
231 these are indeed spatially correlated ([figure -9](#)) with high level of statistical significance. Figure  
232 -9a) shows the correlation of SST and CO<sub>2</sub> over the entire globe and 9b shows T –value for  
233 significance test of these correlation. It clearly implies that over North Indian Ocean the SST  
234 is highly correlated with the CO<sub>2</sub> and therefore it could be one of the key factor controlling the

235 ocean heat. The trend of increasing cyclones after 2011 is effect of increased OHC  
236 corresponding to an enhanced ocean carbon content.

237 Apart from these local characteristics and their impact on cyclogenesis, North Indian Ocean  
238 (NIO), is known for getting boosts of ocean heat and energy from Southern Indian Ocean.  
239 [Bhowmick et al 2019](#) has shown that BOB receives extra shots of heat energy during La-Niña  
240 years from the Western Pacific via south eastern Indian Ocean. Thus we cannot rule out a  
241 similar possibility for AS. Being in close proximity to AS, SWIO can extend its influence  
242 remotely over AS. However, these two areas are known to be separated by the strong equatorial  
243 currents. Also, since the spatial distance is much between the two, it is required to observe the  
244 heat content of this region prior to the post-monsoon. Hence, we observed the OHC of SWIO  
245 between Mays to Septembers. The [figure10](#) shows the OHC in SWIO along 10S. Very clearly  
246 after 2011 there was normal variability in the OHC of this area with usual modulation by El-  
247 Niño and La-Niña events along with positive and negative phases of IOD. Between 2011 -2017  
248 there is a peak in OHC during 2015 followed by 2014 and 2011 where the ACE of AS also  
249 increases significantly.

250 However, before drawing an inference about influence of OHC of SWIO on AS cyclones it is  
251 necessary to analyse the way this heat gets into AS since there is strong equatorial current that  
252 stands in between. Therefore, the meridional transport of heat along the equator is analysed  
253 and is shown in [Figure 11](#). It in general speaks about the kind of heat exchanges between AS  
254 and SWIO. In September and October, the meridional heat transfer is negative implying a  
255 southward propagation of heat, where the AS loses heat to SWIO. On the other hand, during  
256 November and December it is positive, meaning AS gaining heat from SWIO. After November  
257 2007 we see a persistent positive transport of heat to AS from SWIO. Very clearly from this  
258 plot it can be seen that 2011 onwards the meridional transport for November and December  
259 between SWIO and AS is a northward propagation of the heat and energy and this exchange  
260 has increased. In all the exceptional years like 2011, 2014 and 2017, AS was heat-fed from  
261 SWIO. Even 2015 have got a fair supply of heat energy during November and December. The  
262 years 2003 and 2004 was having an upper ocean heat content of similar magnitude, however  
263 the 2004 was significantly more fresh and stratified than 2003. This ideally should imply a  
264 larger heat content for 2004 which however was not observed. This is typically because in 2004  
265 the meridional heat transport from September-November was negative draining out heat from  
266 AS. However, 2004 has seen a significant ACE predominantly due to local freshening impact.  
267 2003 on the other hand had got a fair supply of heat with positive meridional transport from  
268 SWIO (which was warmer in 2003) contributing for a decent ACE. Between 1992 to 1998 the  
269 ACE of AS was maintained without much variability. The OHC in this phase was also similar  
270 except large values in 1997 which is attributed to low upper ocean salinity. However, in 1997  
271 most AS heat was transported towards south, making the available ocean energy for cyclone  
272 comparable with other years between 1992-98. Years 1992, 1994, 1995 and 1998 shows very  
273 large OHC in SWIO, but there was only significant meridional transport in 1992 and 1998.

274 Heat exchanges between AS and SWIO however can never happen unless the intermediate  
275 currents facilitate such exchanges. We analyse the inter-annual variation of zonal and  
276 meridional currents as shown in [figure12](#). These are 700m average zonal and meridional  
277 currents along the equator. Very clearly the years which are having a higher meridional  
278 transport towards AS from SWIO are accompanied by a weakening of the zonal currents in the  
279 post monsoon months between September to November.

280 Thus, it can be inferred that from ocean point of view, AS cyclones are correlated to ocean heat  
281 content (OHC). The OHC is controlled by complicated combination of two factors. Firstly,  
282 local factor in which OHC of AS is found to be modulated by the increasing carbon content of

283 ocean and variability of salinity. Secondly there is remote influence of heat exchanges that  
284 takes place between AS and SWIO. This heat exchange is driven by post-monsoon meridional  
285 heat transport and is facilitated by weakening of the zonal equatorial currents.

## 286 **5. Conclusion**

287 Long term variability of accumulated cyclone energy (ACE) over Arabian Sea (AS) during the  
288 post monsoon month is analysed using cyclone records from JTWC. This is done from oceanic  
289 perspective. Records indicate that there are discrete phases of cyclonic activities over AS. Short  
290 spells of activity are from 1992-1998 and 2003-2004. Monotonic rise in AS cyclones is  
291 observed from 2011 onwards. In this study role of ocean parameters towards modulation of  
292 cyclone variability is studied. Ocean Heat Content (OHC) is found to play a critical role. The  
293 study shows, OHC over AS, is mostly governed by amalgamation of two factors. One of them  
294 is local and the other is a remote ocean process.

295 A reduced salinity due to good monsoon rainfall traps heat in upper parts of the ocean due to  
296 stratification, increasing the OHC. This is the first local process. Further, after 2011 the  
297 monotonic enhancement of partial pressure of carbon is found to be highly correlated to the  
298 SST of AS and therefore certainly modulates the local OHC.

299 When we discuss the remote impact, heat exchanges between AS and South Western Indian  
300 Ocean (SWIO) is important. We systematically examined these exchanges in light of  
301 intermediate equatorial currents. In many years the SWIO is contributing towards the heat  
302 content of AS promoting cyclonic activities, while in some years we find AS drains its heat to  
303 SWIO. This happens through meridional heat transport between them. The analysis of zonal  
304 and meridional current shows that the exchange of this heat is facilitated by weakening of the  
305 zonal equatorial currents during Novembers and Decembers. Thus apart from the atmospheric  
306 parameters, it is important to carefully consider the ocean salinity, heat content and transport  
307 between AS and SWIO for better predictability of the cyclones over this region.

## 308 **6. Acknowledgements**

309 We would like to sincerely thank the Director, Space Applications Centre (SAC), Deputy  
310 Director EPSA/SAC, Group Director AOSG/EPASA/SAC for motivation and support. We are  
311 extremely grateful to Head, OSD(E) for her encouragement. *In situ* data used in this work has  
312 been provided by INCOIS, Hyderabad.

## 313 **Declarations**

314 **Funding:** No funding

315 **Conflicts of interest/Competing interests:** Not Applicable

## 316 **Authors' contributions**

317 Suchandra A Bhowmick: Concept, experiment, analysis and writing.

318 Anup Mandal: Experiment and writing

319

320 **References:**

- 321 Akhil, V., Durand, F., Lengaigne, M. and Vialard, J., (2014) A modeling study of the  
322 processes of surface salinity seasonal cycle in the Bay of Bengal JGR: Atmosphere doi:  
323 10.1002/2013JC009632  
324
- 325 Ali MM, Jagadeesh PSV, Jain S (2007) Effects of eddies and dynamic topography on  
326 the Bay of Bengal cyclone intensity. EOS Trans AGU 88(8):93–95  
327
- 328 Ali MM, Kashyap T, Nagamani PV (2013) Use of sea surface temperature for cyclone  
329 intensity prediction needs a relook. EOS 94:117  
330
- 331 Balmaseda MA, Mogensen K, Weaver A (2013) Evaluation of ECMWF ocean  
332 reanalysis system ORAS4. QJRM,139(674):1132–1161  
333
- 334 Bhowmick S. A, Agarwal N, Ali M.M, Kishtawal C.M. and Sharma R. (2019), Role of  
335 ocean heat content in boosting post-monsoon tropical storms over Bay of Bengal during  
336 La-Niña events, *Climate Dynamics*, 52: 7225-7234, DOI 10.1007/s00382-016-3428-5.  
337 Dee, DP, Uppala. SM, Simmons AJ, Berrisford P, Poli P, Kobayashi S, Andrae U,  
338 Balmaseda MA, Balsamo G, Bauer P, Bechtold P, Beljaars ACM, van de Berg L, Bidlot  
339 J, Bormann N, Delsol C, Dragani R, Fuentes M, Geer AJ, Haimberger L, Healy SB,  
340 Hersbach H, Hólm EV, Isaksen L, Kóallberg P, Köhler M, Matricardi M, McNally  
341 AP, Monge-Sanz BM, Morcrette J-J, Park B-K, Peubey C, de Rosnay P, Tavolato C,  
342 Thépaut J-N, Vitart F. (2011), The ERA-Interim reanalysis: configuration and  
343 performance of the data assimilation system. *Q. J. R. Meteorol. Soc.* 137: 553–597.  
344 DOI:10.1002/qj.828  
345
- 346 Evan, A.T and Camargo S.J. (2011). A climatology of Arabian Sea Cyclonic Storms,  
347 *Journal of Climate* Vol 24, 1, 140-158.  
348
- 349 Goni GJ, Trinanes JA (2003) Ocean thermal structure monitoring could aid in the  
350 intensity forecast of tropical cyclones. EOS Trans AGU 84(51):573  
351
- 352 Häkkinen S, Rhines PB, Worthen DL (2016) Warming of global ocean: spatial  
353 structures and water mass trends. *J Clim* 29:4949–4963  
354
- 355 Landschützer, P., N. Gruber and D.C.E. Bakker (2017). An updated observation-based  
356 global monthly gridded sea surface pCO<sub>2</sub> and air-sea CO<sub>2</sub> flux product from 1982  
357 through 2015 and its monthly climatology (NCEI Accession 0160558). Version 2.2.  
358 NOAA National Centers for Environmental Information. Dataset. [2017-07-11]  
359
- 360 Murakami, H., G. A. Vecchi, and S. Underwood, 2017: Increasing frequency of  
361 extremely severe cyclonic storms over the Arabian Sea. *Nat. Clim. Change*, 7, 885-889.  
362
- 363 Murthy, T.S. and El-Sabh. M.I. Cyclones and storms surges in Arabian Sea: A brief  
364 review, DSR, Vol 31, 6-8, 665-670,1984.  
365
- 366 Prasanna Kumar, S. Roshin R.P, Navvekar J, Kumar P.K.D, Vivekanandan, E, (2009)  
367 Response of the Arabian Sea to global warming and associated regional climate shift,  
368 *Marine Environmental Research* 68, 217-222.

369  
370  
371  
372  
373  
374  
375  
376  
377  
378  
379  
380  
381  
382  
383  
384  
385  
386  
387  
388  
389  
390  
391  
392  
393  
394  
395  
396  
397  
398  
399  
400  
401  
402  
403  
404  
405  
406  
407  
408  
409  
410  
411  
412  
413  
414  
415  
416  
417  
418

Sahoo, B. and Bhaskaran, PK (2016) Assessment on historical cyclone tracks in the Bay of Bengal, east coast of India. *Int. Journal of climatology* 36(1), pp-95:109.

Sumesh. K.G. and Ramesh Kumar, M.R. Tropical cyclones over North Indian Ocean during El-Nino Modos Years, *Natural Hazards* 68,1057-1074, 2013

Shay LK, Goni GJ, Black PG (2000) Effects of a warm oceanic feature on Hurricane Opal. *Mon Weather Rev* 128(5):1366–1383

Sattar, A. M., & Cheung, K. K. W. (2019). Comparison between the active tropical cyclone seasons over the Arabian Sea and Bay of Bengal. *International Journal of Climatology*, 39(14), 5486-5502. <https://doi.org/10.1002/joc.6167>

419

**Figure and Tables**

420 *Table -1a: The El-nino/La-nina events were categorized from Oceanic Nino Index (ONI)*

<b>ONI &gt; 0.5</b>	<b>1982,1986,1987,1991,1994,1997,2002, 2004,2006,2009,2014,2015,2018</b>
<b>ONI &lt; -0.5</b>	<b>1983,1984,1988,1995,1998,1999,2000, 2005,2007,2008,2010,2011,2016,2017</b>
<b>-0.5 &lt; ONI &lt; 0.5</b>	<b>1979,1980,1981,1985,1989,1990,1992, 1993,1996,2001,2003,2012,2013,2019</b>

421

*Table -1b: The Indian Ocean Dipole (IOD) conditions in different years*

<b>Positive IOD years</b>	<b>Negative IOD years</b>
<b>1982,1983,1994,1997, 2006,2012,2015,2019</b>	<b>1981,1989,1992,1996, 1998,2010,2014,2016</b>

422

423

424

425

426

427

428

429

430

431

432

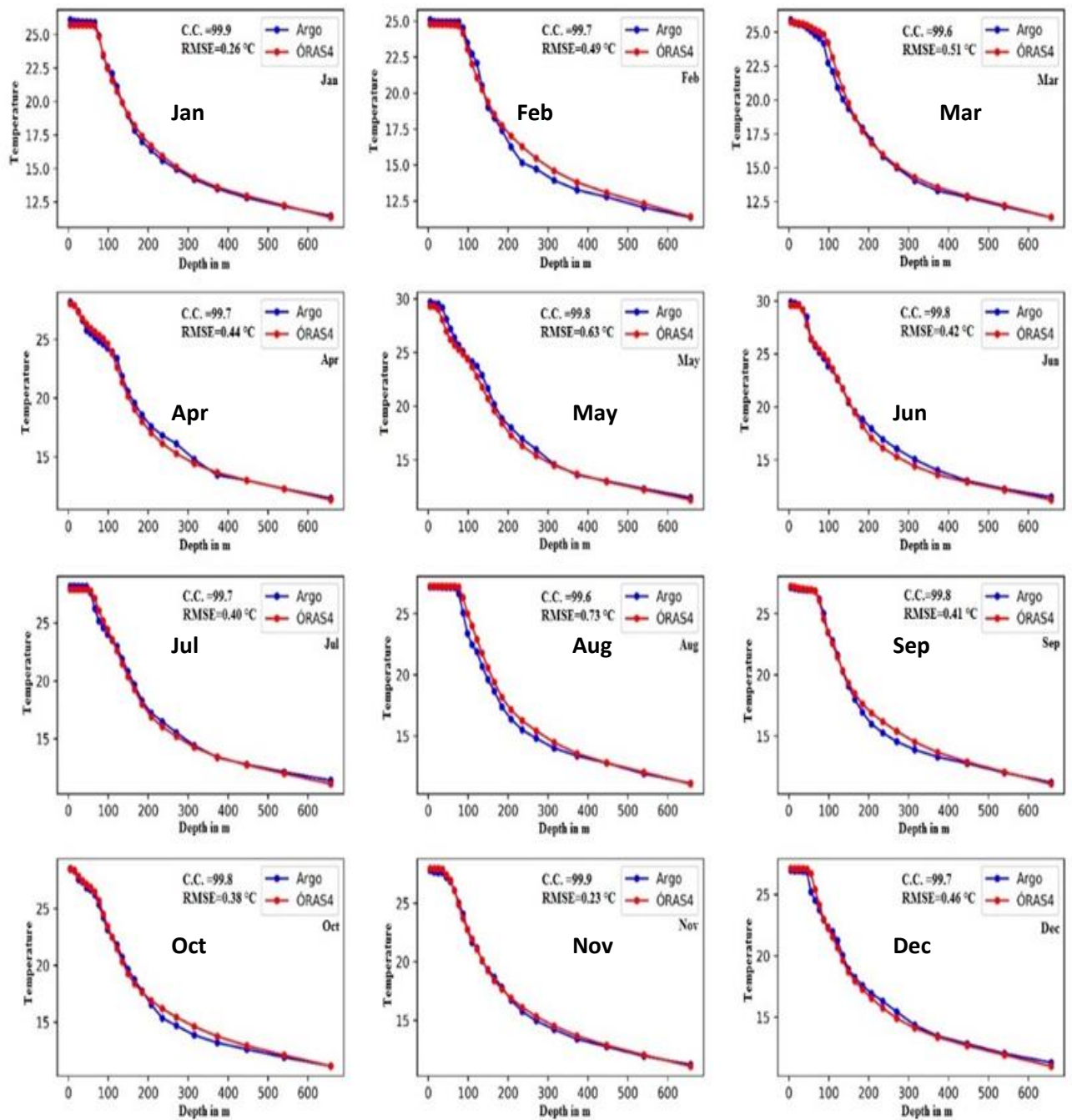
433

434

435

436

437



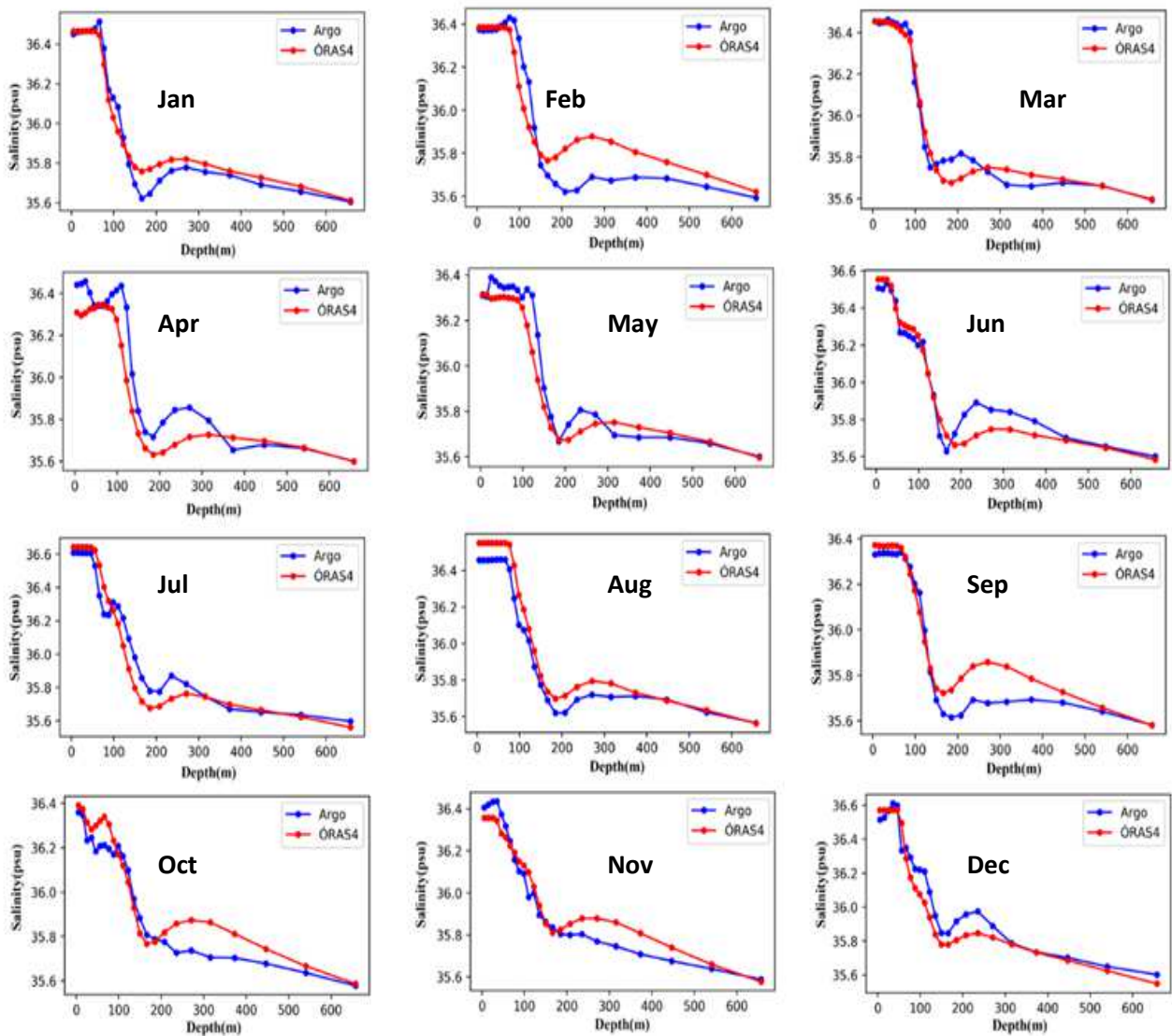
439 Figure-1 The Comparison of the ORAS4 temperature profile with an Argo measurement over  
 440 Arabian Sea for 2012

441

442

443

444



446 Figure-2 The Comparison of the ORAS4 salinity profile with an Argo measurement over  
447 Arabian Sea for 2012

448

449

450

451

452

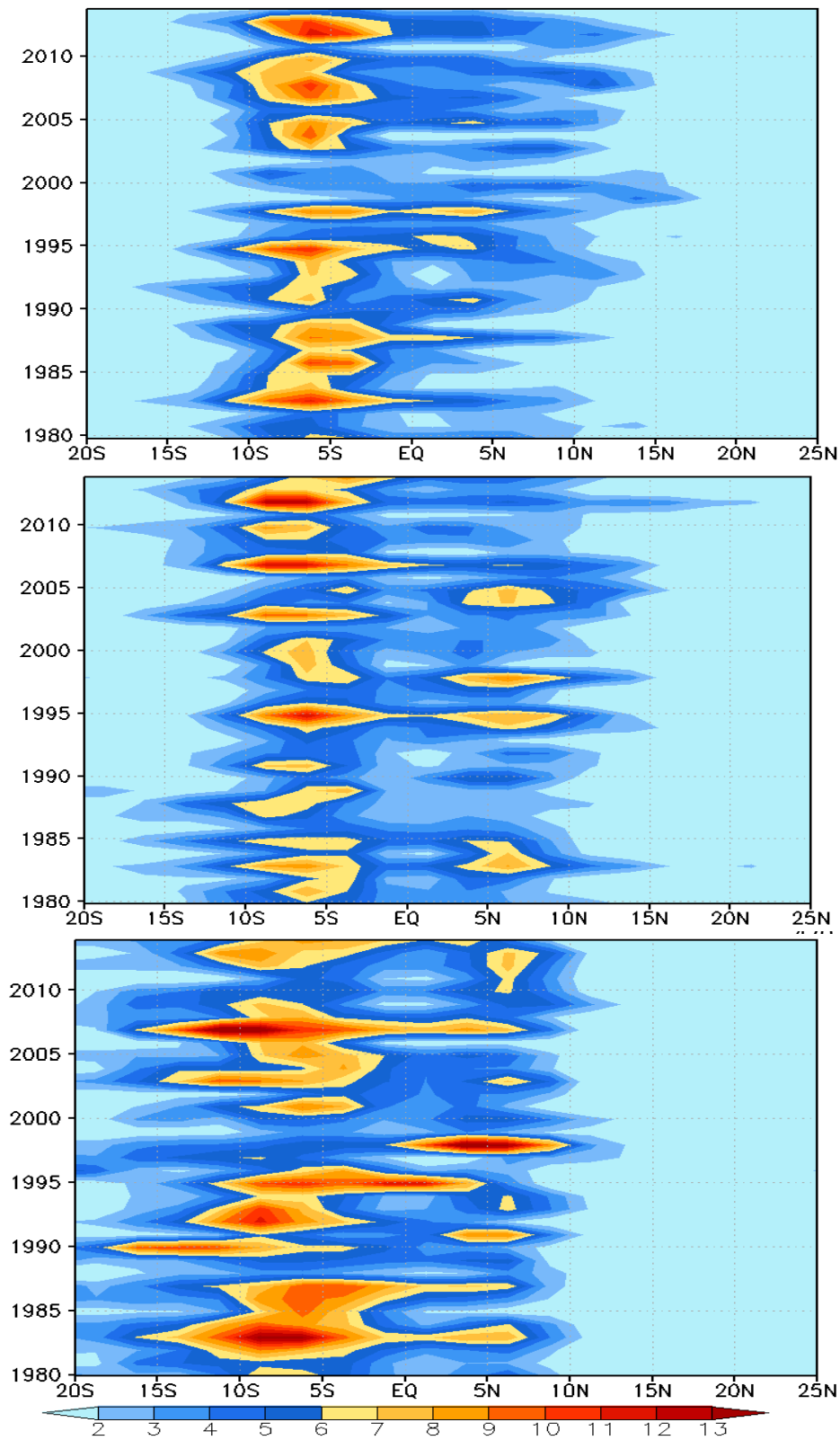
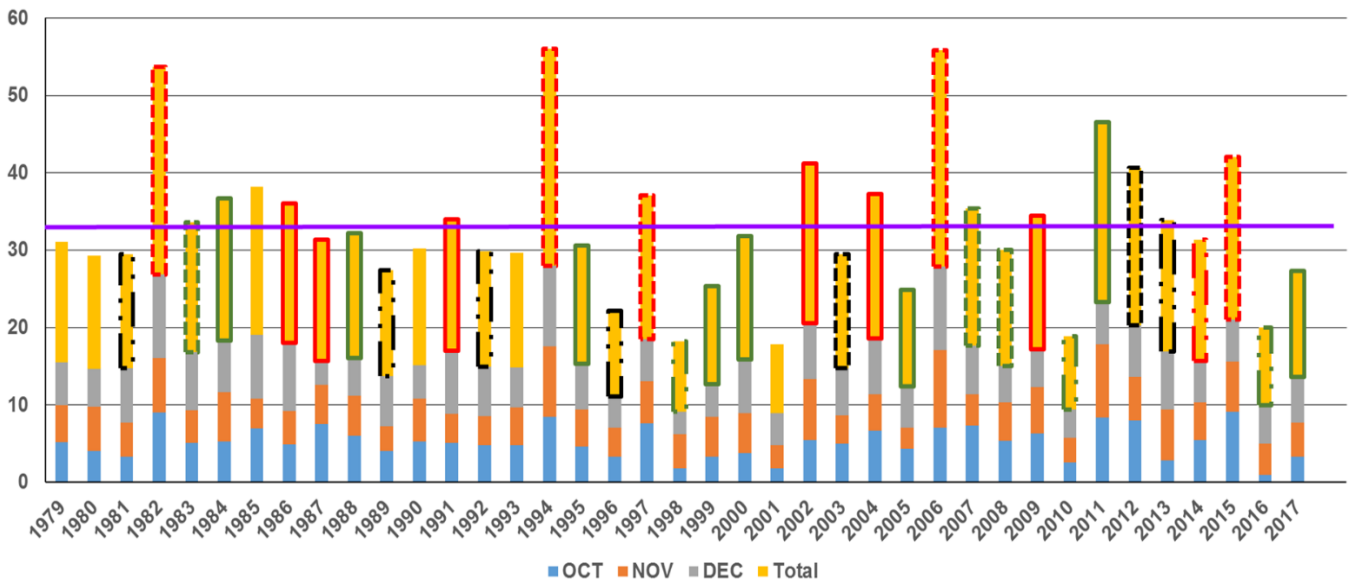


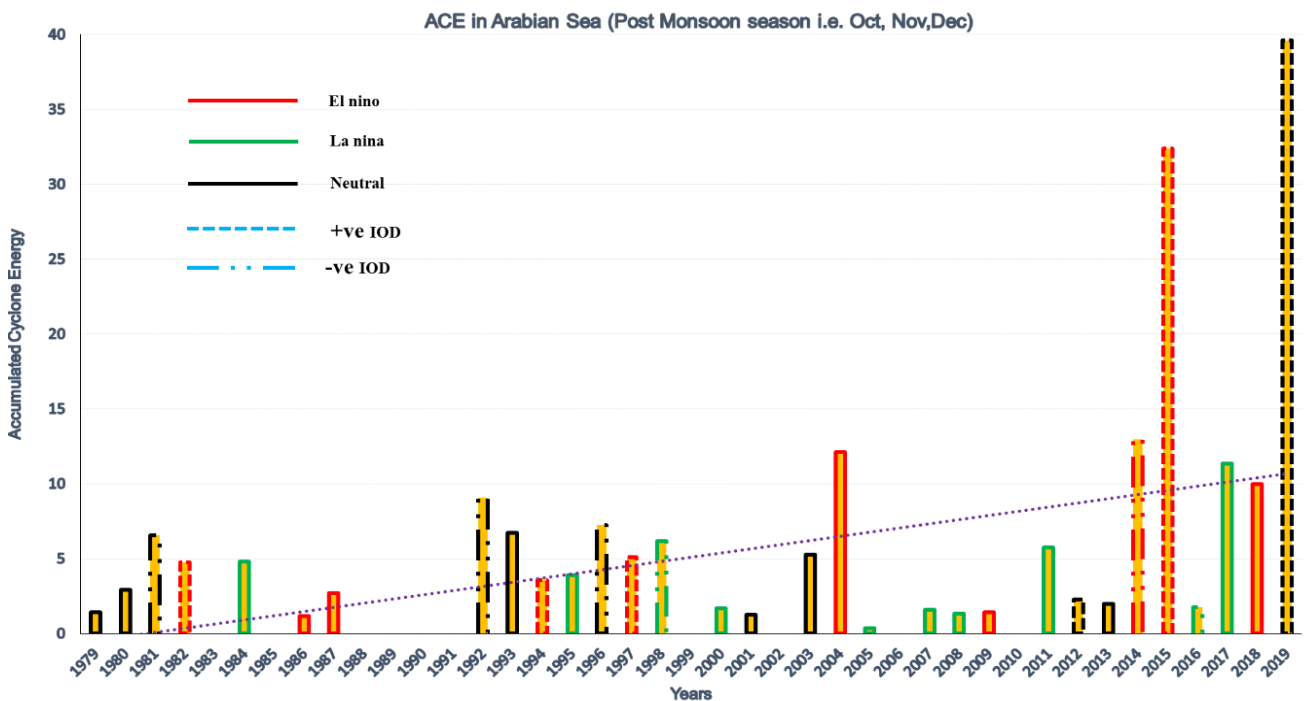
Figure-3: Inter-annual variation of average monthly rate of precipitation (mm/day) from CPC Merged Analysis of Precipitation (CMAP) averaged between 50°-70°E i.e. over Arabian sea

480



481 Figure- 4 Inter-annual variation of average monthly rate of precipitation (mm/day) from CPC  
482 Merged Analysis of Precipitation (CMAP) averaged between 50°-70°E and 0-10°S

483

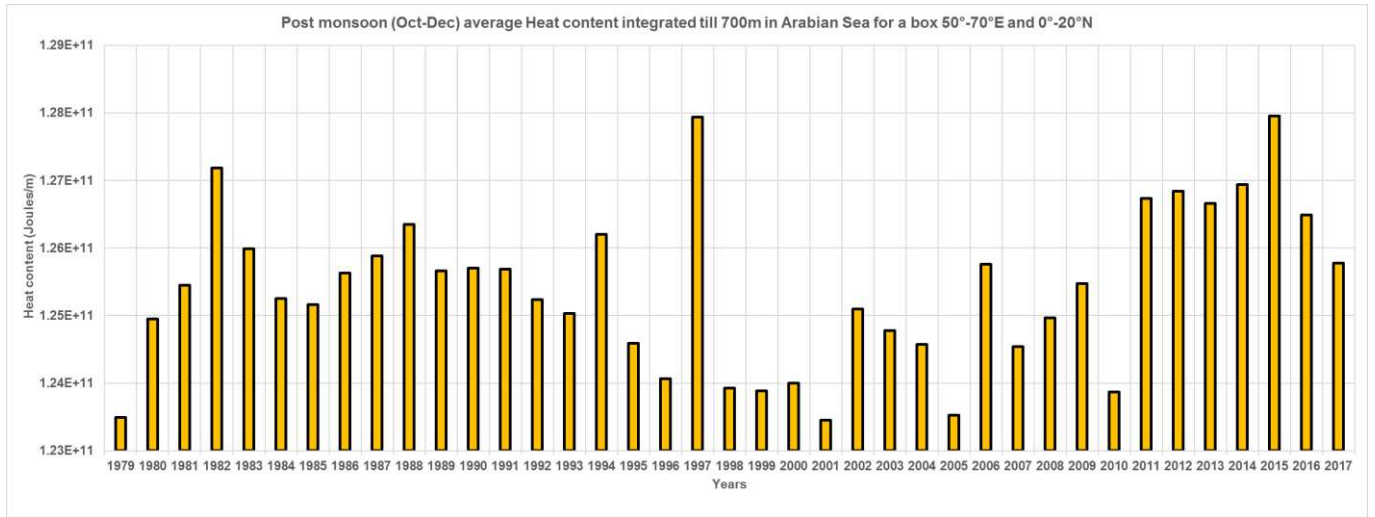


484 Figure-5 Accumulated cyclone energy from 1979-2019. Years are classified into the El-Niño,  
485 La-Niña, positive and negative IOD years.

486

487

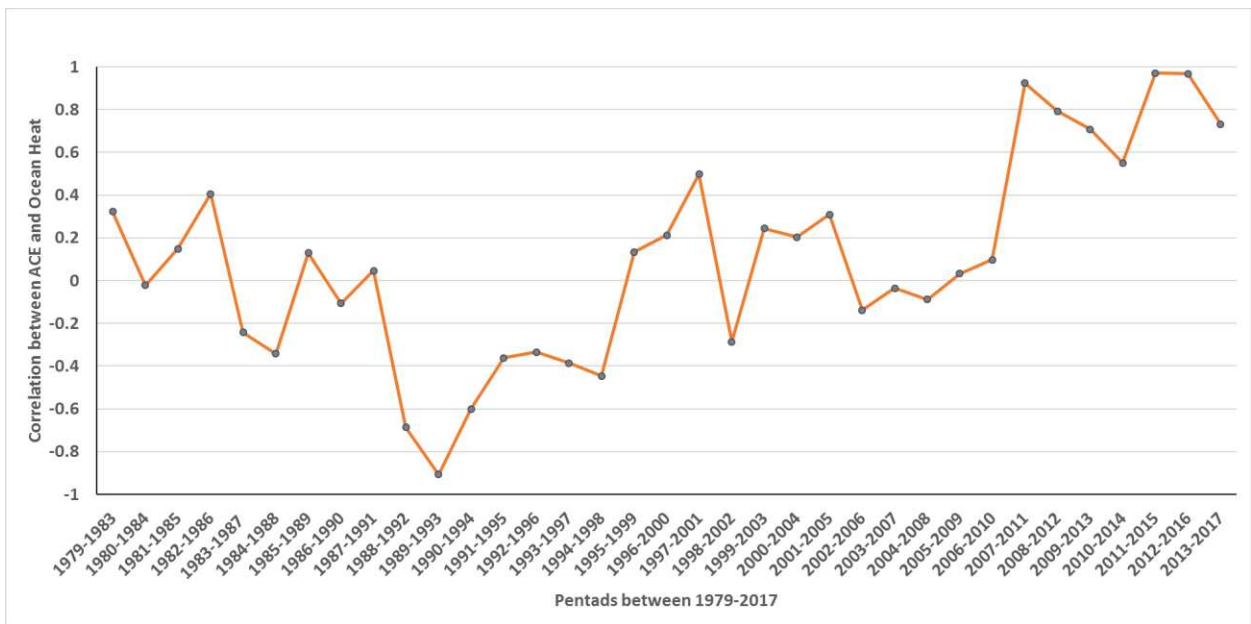
488



489 Figure-6a Inter-annual variation of post-monsoon average heat content over AS integrated up  
 490 to 700m for a box between 50-70°E and 0-20° N

491

492



493

494 Figure-6b Variation of correlation coefficient between OHC over AS integrated up to 700m  
 495 for a box between 50-70°E and 0-20° N and ACE.

496

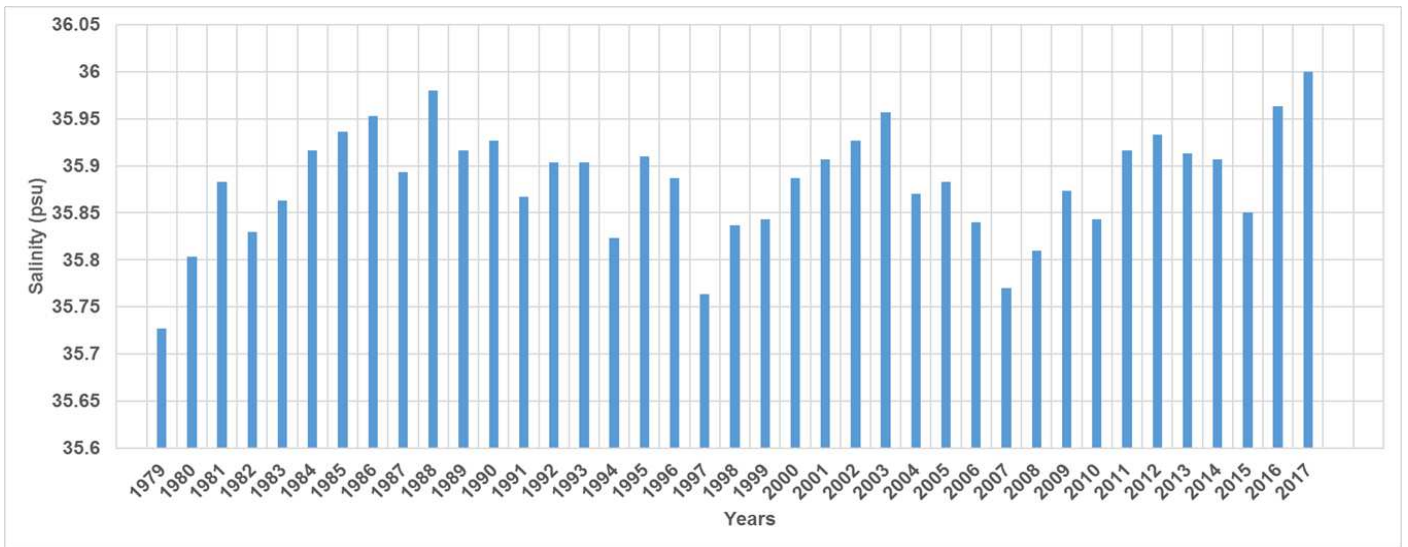
497

498

499

500

501



502

503

Figure 7 The variation of salinity averaged up to 100m for the same box.

504

505

506

507

508

509

510

511

512

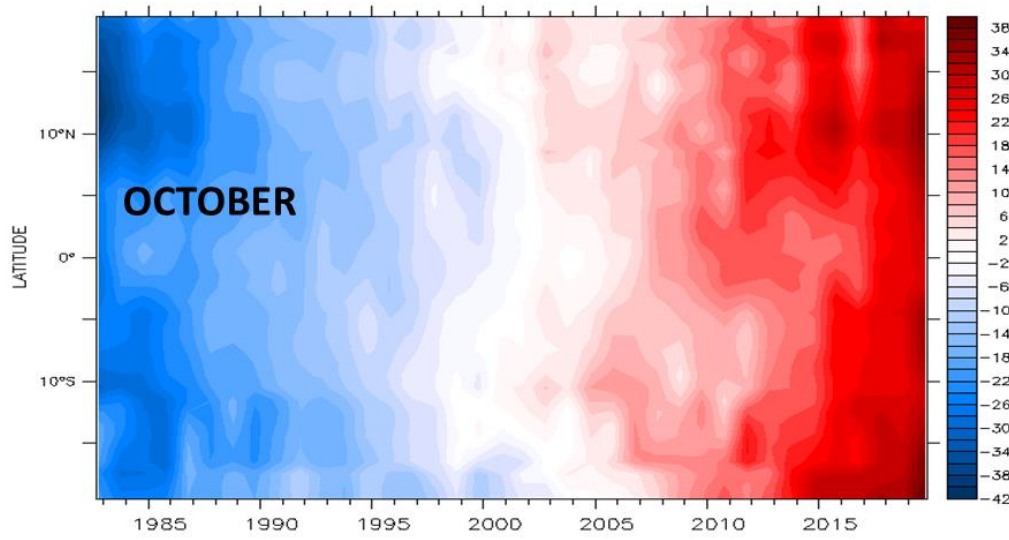
513

514

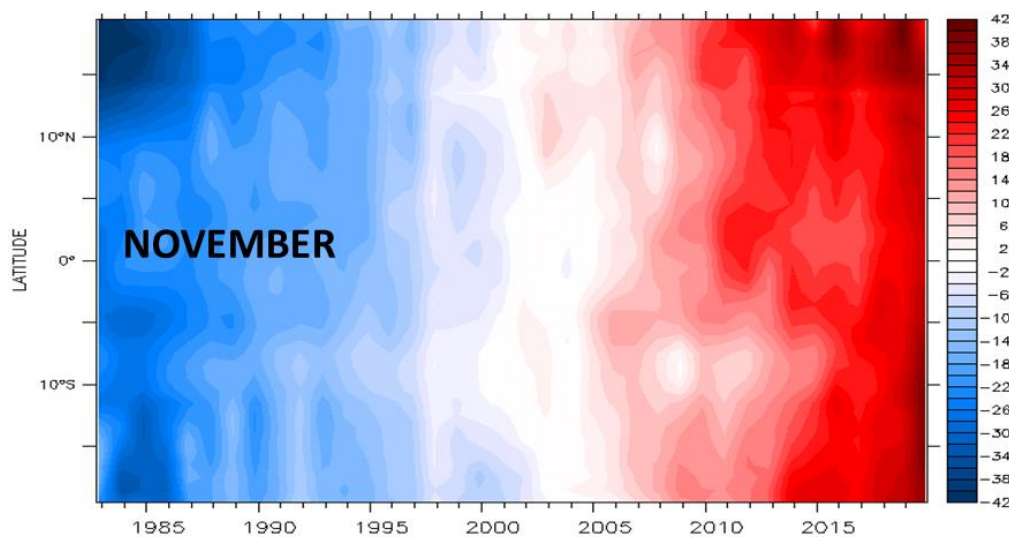
515

516

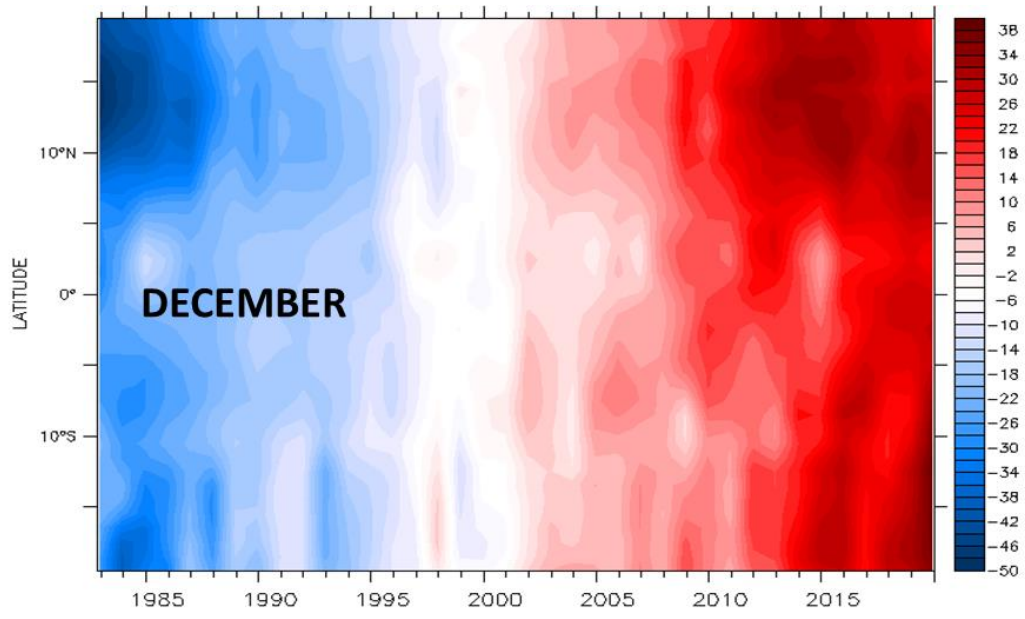
517



518

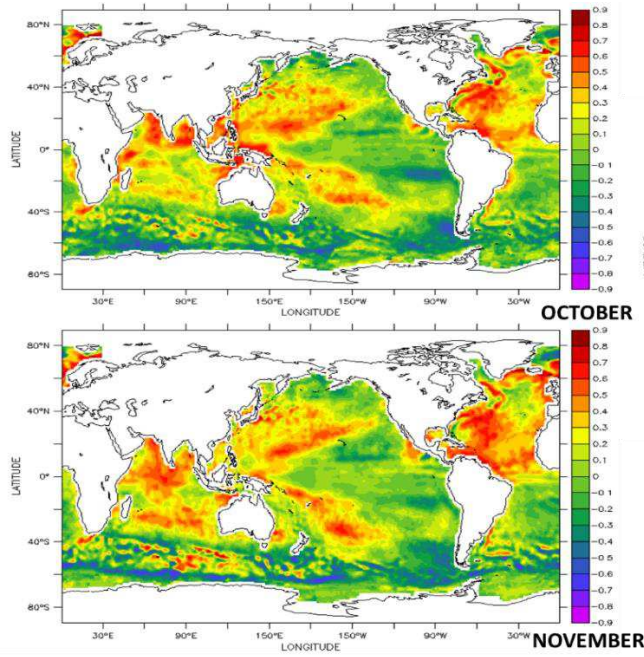


519

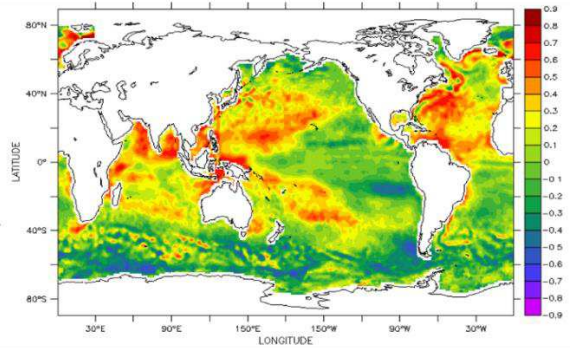


520

521 Figure 8 The variation of anomaly in partial pressure of carbon at surface between 50-70E  
 522 from 1982-2019.



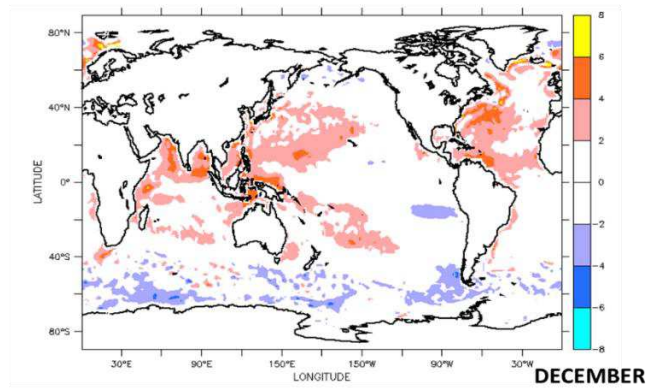
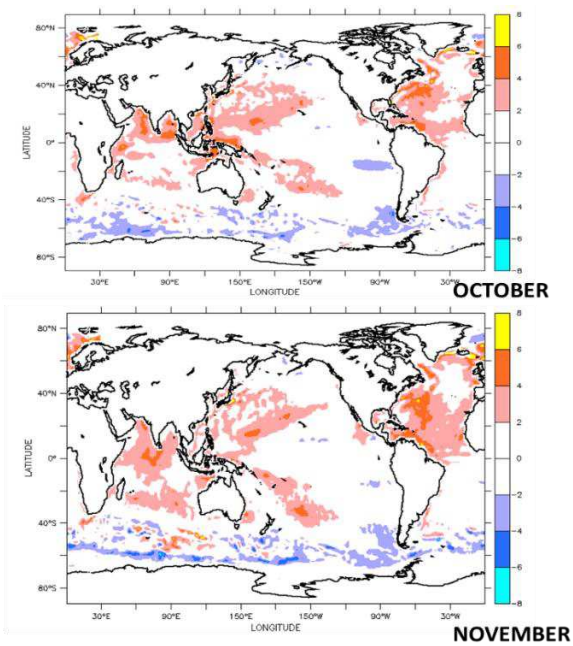
The Correlation Of Global Sea Surface Carbon and SST



Data 1982-2018 ERA Interim SST and observation based gridded monthly SPCO2

523

524



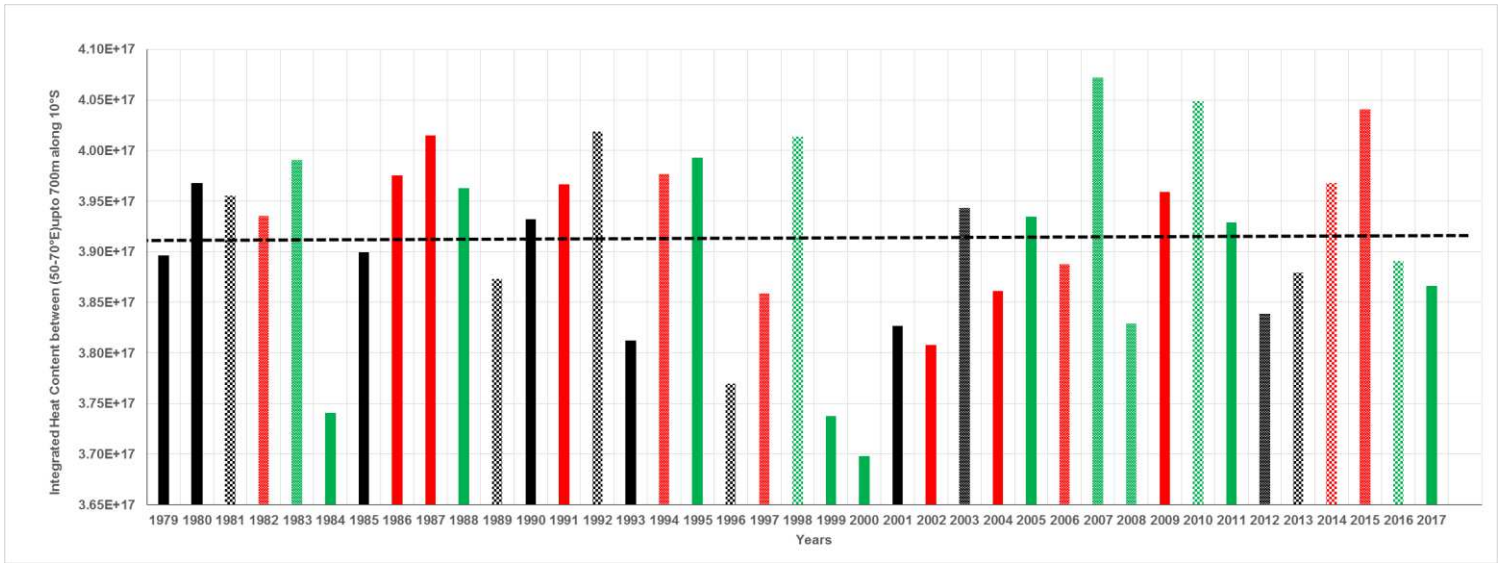
The T-Value of correlation between Sea Surface Carbon and SST

525

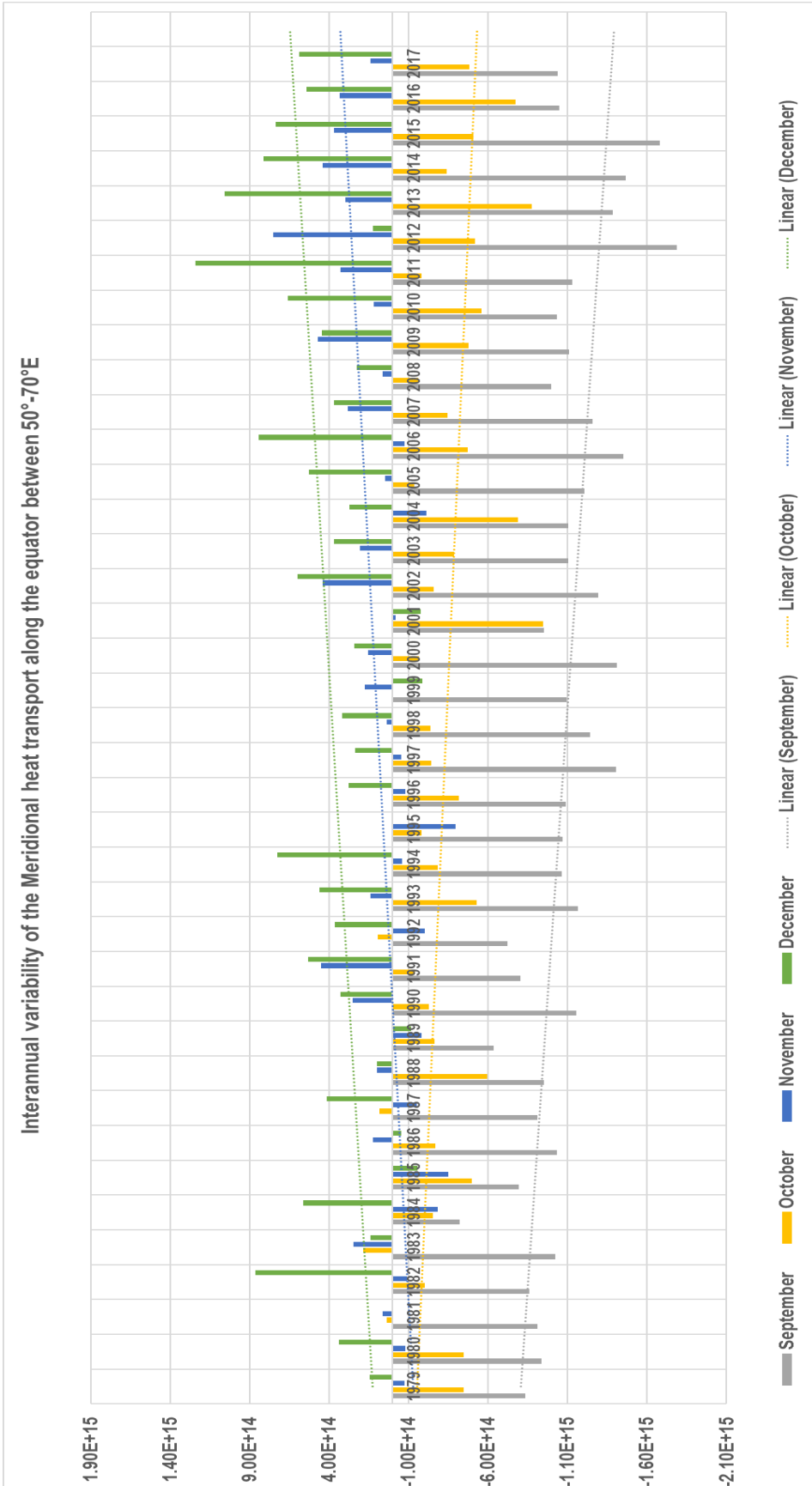
526 Figure 9 (a) Correlation coefficient between partial pressure of carbon at surface and SST for  
 527 global ocean 1982-2019 (b) Statistical significance of the correlation (T value).

528

529



531 Figure-10 The integrated heat content between 50-70E integrated up to 700m along 10S



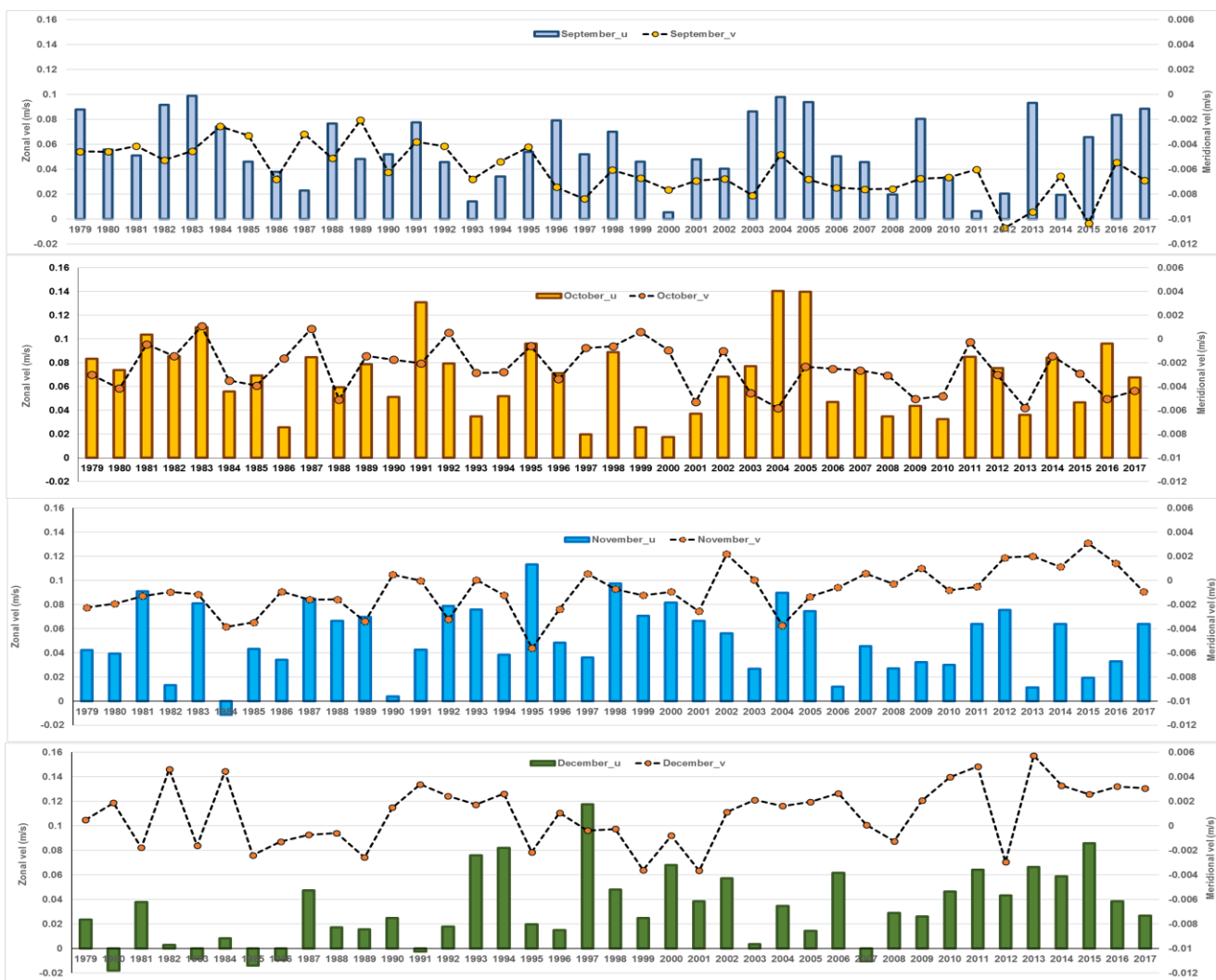
532

533

534

Figure-11 the inter-annual variability of the meridional heat transport along equator integrated up to 700 m

535



536

537 Figure-12 the inter-annual variability of the zonal (bar)/meridional(line) currents at equator  
538 up to 700 m

539

540

541

542

543

544